

# Exciton spin dynamics of colloidal CdTe nanocrystals in magnetic field

Feng Liu,<sup>1</sup> A. V. Rodina,<sup>2</sup> D. R. Yakovlev,<sup>1,2</sup> A. Greilich,<sup>1</sup> A. A. Golovatenko,<sup>2,3</sup>  
A. S. Susha,<sup>4</sup> A. L. Rogach,<sup>4</sup> Yu. G. Kusrayev,<sup>2</sup> and M. Bayer<sup>1,2</sup>

<sup>1</sup>*Experimentelle Physik 2, Technische Universität Dortmund, 44221 Dortmund, Germany*

<sup>2</sup>*Ioffe Physical-Technical Institute, Russian Academy of Sciences, 194021 St. Petersburg, Russia*

<sup>3</sup>*St. Petersburg National Research University ITMO, 197101 St. Petersburg, Russia. and*

<sup>4</sup>*Department of Physics and Materials Science, City University of Hong Kong, Hong Kong S.A.R.*

(Dated: September 27, 2018)

The recombination and spin dynamics of excitons in colloidal CdTe nanocrystals (NCs) are studied by time-resolved photoluminescence in high magnetic fields up to 15 T and at cryogenic temperatures. The recombination decay shows a nonexponential temporal behavior, with the longest component corresponding to the dark excitons having 260 ns decay time at zero magnetic field and 4.2 K temperature. This long component shortens to 150 ns at 15 T due to the magnetic-field-induced mixing of the bright and dark exciton states. The spin dynamics, assessed through the evolution of the magnetic-field-induced circular polarization degree of the photoluminescence, has a fast component shorter than 1 ns related to the bright excitons and a slow component of 5-10 ns associated with the dark excitons. The latter shortens with increasing magnetic field, which is characteristic for a phonon-assisted spin relaxation mechanism. The relatively low saturation level of the associated magnetic-field-induced circular polarization degree of  $-30\%$  is explained by a model that suggests the CdTe NCs to constitute an ensemble of prolate and oblate NCs, both having a structural quantization axis. The exciton  $g$ -factor of 2.4-2.9 evaluated from fitting the experimental data in the frame of the suggested approach is in good agreement with the expected value for the dark excitons in CdTe NCs.

PACS numbers: 73.21.La, 78.47.jd, 78.55.Et, 78.67.Hc

## I. INTRODUCTION

Colloidal thiol-capped CdTe nanocrystals (NCs) are well known example of the colloidal quantum dots directly synthesized in aqueous solution [1–4]. Due to the great variety of surface functionalities offered by various thiols, which can be as capping molecules at the synthetic stage, a large variety of composite materials employing this kind of nanocrystals as building blocks can be designed. Due to their high photoluminescence quantum yields these NCs have found applications in various fields ranging from light harvesting and energy transfer [5] to biotechnology [6–9]. Colloidal NCs have also reached potential applications in the devices exploring the spin degree of freedom [10–12].

The effect of an applied magnetic field on the exciton recombination dynamics has been studied for CdSe [13–16], PbSe [17] and CdTe [18] NCs. The impact is most pronounced at low temperatures, when in equilibrium the dark exciton states are predominantly populated. The recombination dynamics show a fast component contributed by recombination of bright excitons and their fast relaxation to the dark state and a slow component contributed by dark exciton recombination. The magnetic field mixes the bright and dark exciton states, resulting in shortening of the slow decay component and vanishing of the fast component. This characteristic behavior in magnetic field looks similar to the behavior induced by a temperature increase due to thermal population of the bright exciton state.

Exciton spin relaxation times have been measured for CdSe NCs in magnetic fields by means of time-resolved

photoluminescence. For neutral NCs the exciton spin dynamics was faster than 1 ns [14–16, 21], while in charged NCs the spin relaxation of the negatively charged exciton can be as long as 60 ns [16]. Time-integrated studies of the magnetic-field-induced circular polarization degree of the exciton emission from CdSe NCs have been reported [19] and it has been also shown that the polarization degrees are similar for isolated NCs and NC aggregates [20]. In CdTe NCs the exciton spin dynamics have not been studied so far.

In this manuscript we report on magneto-optical studies of the recombination and spin dynamics of excitons in an ensemble of colloidal CdTe NCs.

## II. EXPERIMENTALS

The thiol-capped colloidal CdTe NCs with an average core diameter of 3.4 nm were synthesized in water following the method described in Ref. 4. For the optical experiments performed at cryogenic temperatures, a solution of CdTe NCs was drop-cast on a glass slice and dried in air. The glass slice was mounted in a sample holder and inserted into a cryostat equipped with a 15 T superconducting magnet. The magnetic field,  $\mathbf{B}$ , was applied in the Faraday geometry, i.e. it was oriented perpendicular to the glass slice and parallel to the light wave vector. A circular polarizer inserted between the sample and the detection fiber allowed us to analyze the  $\sigma^+$  and  $\sigma^-$  polarization of the emission by inverting the magnetic field direction. The sample was in contact with helium gas so that the bath temperature could be varied from

$T = 4.2$  K up to 300 K.

Photoluminescence (PL) was excited and collected through multimode optical fibers. The collected signal was dispersed with a 0.55 m spectrometer. Time-integrated PL spectra were measured under continuous-wave (CW) laser excitation with a photon energy of 3.33 eV (wavelength 372 nm) and detected with a liquid-nitrogen-cooled charge-coupled-device camera. We denote them as steady-state PL spectra.

For time-resolved measurements the sample was excited by a picosecond pulsed laser (photon energy 3.06 eV, wavelength 405 nm, pulse duration 50 ps, repetition frequency 150 to 500 kHz). Here the PL signal was sent through the spectrometer and detected by an avalanche photodiode (time response 50 ps) connected to a conventional time-correlated single-photon counting module. The instrument response function of the whole setup was limited by the optical fiber dispersion to a resolution of 800 ps. All measurements were performed at low excitation densities of about  $0.1 \text{ mW/cm}^2$  to suppress any multiexciton contributions to the emission spectra.

Analysis of the PL circular polarization degree induced by an external magnetic field is a powerful tool to investigate the spin levels of the exciton complexes, to identify their charging state and to obtain information on the spin dynamics, see, e.g., Refs. [16, 22] and references therein. The degree of circular polarization (DCP) is defined by:

$$P_c(t) = \frac{I^+(t) - I^-(t)}{I^+(t) + I^-(t)}. \quad (1)$$

Here  $I^+(t)$  and  $I^-(t)$  are the  $\sigma^+$  and  $\sigma^-$  polarized PL intensities, respectively, measured at time delay  $t$  after pulsed excitation [23]. A saturation of  $P_c(t)$  at times much longer than the exciton spin relaxation time gives the equilibrium circular polarization degree  $P_c^{eq}(B)$ .

The time-integrated DCP can be evaluated by integrating the corresponding PL intensities over time:

$$P_c^{\text{int}} = \frac{\int dt I^+(t) - \int dt I^-(t)}{\int dt I^+(t) + \int dt I^-(t)}. \quad (2)$$

In case of CW excitation the measured polarization degree corresponds to  $P_c^{\text{int}}$ .

The magnetic-field-induced DCP is caused by exciton thermalization among the Zeeman spin levels. While the equilibrium polarization degree  $P_c^{eq}(B)$  is controlled solely by the thermal equilibrium population of the Zeeman spin levels, the time-integrated polarization  $P_c^{\text{int}}$  depends also on the ratio of the exciton spin relaxation time  $\tau_s$  and the exciton lifetime  $\tau$ :

$$P_c^{\text{int}}(B) = \frac{\tau}{\tau + \tau_s} P_c^{eq}(B). \quad (3)$$

If  $\tau_s \ll \tau$  the experimentally measured  $P_c^{\text{int}}(B)$  coincides with  $P_c^{eq}(B)$ , while otherwise their difference is controlled by the dynamical factor  $d = \tau/(\tau + \tau_s)$ .

The magnetic field dependence of  $P_c^{\text{int}}(B)$  can be rather complicated as  $\tau_s$  and  $\tau$  can also be functions of

magnetic field. In addition, one has to take into account the exciton level degeneracy and exciton fine structure in zero magnetic field, which depends on the crystal symmetry of the semiconductor material and on the nanocrystal shape. In spherical hexagonal CdSe NCs or prolate cubic CdTe NCs the hole states are split by the anisotropy field, and the exciton ground state has angular momentum projections of  $\pm 2$  onto the quantization axis. The exciton Zeeman splitting depends on the angle between the quantization axis and the magnetic field direction. The analysis of DCP for an ensemble of such anisotropic NCs with random orientation of their axes relative to the magnetic field is presented in Refs. [14, 24] for neutral and in Ref. [16] for charged excitons (trions).

Note that in ideally round-shaped NCs with cubic lattice structure there is no preferential structural quantization axis, while such an axis becomes well-defined when the NC shape is deformed to be prolate or oblate and/or for materials with lower crystal symmetry, e.g., wurtzite CdSe. The shape of thiol-capped NCs with cubic-phase zinc blend crystal structure had been determined not to be spherical, but rather tetrahedron or truncated tetrahedron-like [25, 26]. While the symmetry of a tetrahedron is the same as for spherical dots, truncated tetrahedrons can be considered as prolate or oblate particles.

### III. RESULTS

Photoluminescence spectra of the CdTe NCs measured under unpolarized CW excitation are shown in Fig. 1(a). At zero magnetic field the PL spectrum has its maximum at 1.988 eV with a full width at half maximum (FWHM) of 120 meV, caused by the NCs size dispersion.

In an external magnetic field the PL becomes circularly polarized with an intensity redistribution in favor of the  $\sigma^-$  component, i.e. the sign of the circular polarization degree defined by Eq. (2) is negative. The polarization is caused by exciton thermalization among the Zeeman spin-split levels. At the PL maximum it reaches a value of  $P_c^{\text{int}} = -0.28$  at  $B = 15$  T.  $P_c^{\text{int}}$  varies only little across the emission band as shown in Fig. 1(b), with some small increase at the high energy tail of the PL spectrum and in magnetic fields exceeding 6 T.

The magnetic field dependences of the spectrally- and temporally-integrated DCP measured under CW excitation at three different temperatures are given in Fig. 1(d). They show the typical behavior for magnetic-field-induced DCP with a linear increase in low magnetic fields and saturation in the high magnetic field limit, as clearly seen for  $T = 4.2$  K. The decrease of the DCP at elevated temperatures is also typical, as the occupation of Zeeman levels is controlled by the ratio of Zeeman splitting to thermal energy  $k_B T$  [16, 27]. As one can see from Eq. (3), the DCP depends both on the dynamical factor  $\tau/(\tau + \tau_s)$  and on the equilibrium polarization  $P_c^{eq}(B)$ . The time-resolved experiments presented below

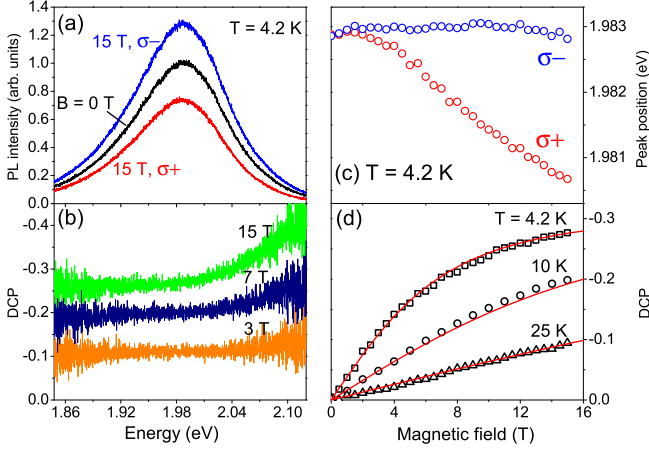


FIG. 1: (a) PL spectra of 3.4 nm CdTe NCs at  $B = 0$  (black) and 15 T (red for  $\sigma^+$  polarization and blue for  $\sigma^-$ ). (b) Spectral dependence of DCP at  $B = 3, 7$  and 15 T and  $T = 4.2$  K. (c) Magnetic field dependence of peak energies of the  $\sigma^+$  and  $\sigma^-$ -polarized components of the PL spectrum. (d) Magnetic field dependence of the spectrally- and temporally-integrated DCP measured at  $T = 4.2, 10$  and 25 K. Lines are fits using Eqs. (8) and (9) with  $g_F = 2.4$  and 2.9, respectively. The fits performed along the two equations coincide with each other to high accuracy and, therefore, are shown by a line for each temperature data set.

show that for the studied CdTe NCs  $\tau_s \ll \tau$  and, therefore, the experimentally measured  $P_c(B)$  corresponds to  $P_c^{eq}(B)$ .

Figure 1(c) shows the magnetic field dependences of the PL peak energies of the  $\sigma^+$  and  $\sigma^-$  polarized spectra. The energy splitting between them reaches 2.3 meV at  $B = 15$  T. Here it is unusual that the  $\sigma^-$  component with stronger intensity is higher in energy. Such a behavior has been observed also for CdSe NCs [15, 19], but a plausible explanation is still missing and further studies are needed to clarify that.

Let us first present the experimental data for the exciton recombination dynamics. In order to avoid the consideration of effects related to spectral diffusion caused by Förster resonant energy transfer (FRET) among the NCs, we measured the spectrally-integrated recombination dynamics in the CdTe NCs, see Fig. 2. It is known, that FRET modifies the spectral dependences of the emission dynamics [28–31]. A similar behavior has been also found for the studied sample and will be reported elsewhere [32].

At zero magnetic field and  $T = 4.2$  K the exciton PL dynamics shown in red in Fig. 2 has a multiexponential decay. The fast initial component with a decay time of 2 ns corresponds to the lifetime of the bright (i.e. optically allowed in the electric-dipole approximation) excitons  $\tau_A$ . This time is contributed by radiative recombination and exciton thermalization from the bright into the dark state. The slow component with a time of about 260 ns corresponds to the lifetime of the

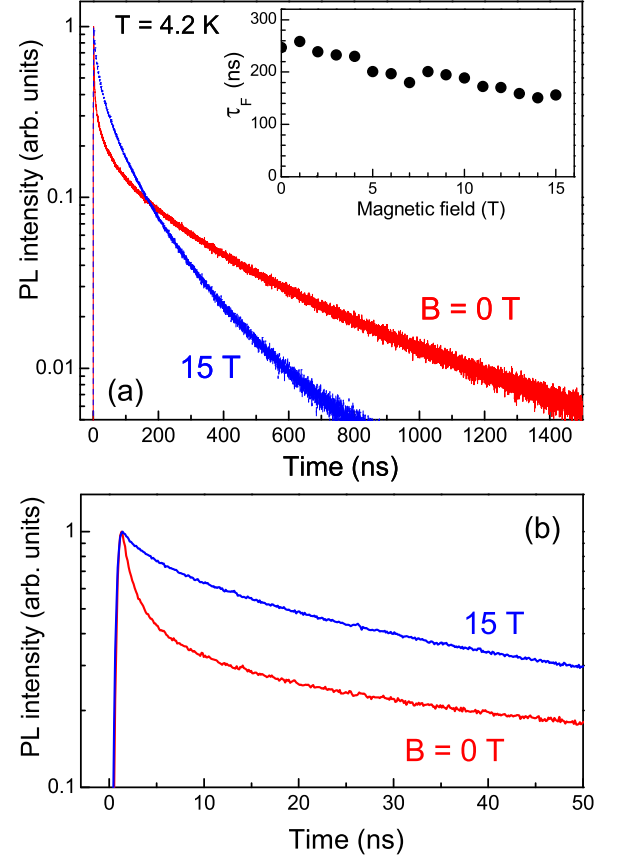


FIG. 2: (a) Dynamics of spectrally-integrated PL intensity of 3.4 nm CdTe NCs measured at zero and 15 T magnetic field. The initial dynamics after pulsed excitation are given in more detail in panel (b). The magnetic field dependence of the recombination time of the slow component is shown in the insert.

dark (optically forbidden) excitons  $\tau_F$ , whose recombination becomes partially allowed due to a weak mixing of dark and bright exciton states caused, e.g., by NC imperfections and surface states. Note, that the PL intensity of the slow component appears to be smaller than that of the fast component, but integrated over time it actually provides the dominant contribution to the overall emission.

With increasing magnetic field up to 15 T the slow decay component continuously shortens from 260 down to 150 ns, see blue curve in Fig. 2(a) and insert. The fast component simultaneously decreases until it vanishes. The PL decay then still cannot be described by a single exponential decay, but its initial part shows a decay with 50 ns characteristic time, considerably longer than the 2 ns at zero magnetic field, see Fig. 2(b). This behavior is typical for colloidal NCs and is due to magnetic-field-induced mixing of bright and dark exciton states [14, 15, 18]. The mixing takes place only in NCs with symmetry further reduced by the magnetic field, i.e., in NCs where the field is not parallel to the spin quantization axis. From the strong magnetic field effect on the re-

combination dynamics shown in Fig. 2, we conclude that the dominant fraction of NCs in the ensembles deviates from the ideal spherical shape so that it has a quantization axis. This conclusion, as will be discussed below, is supported by the results of polarized PL experiments.

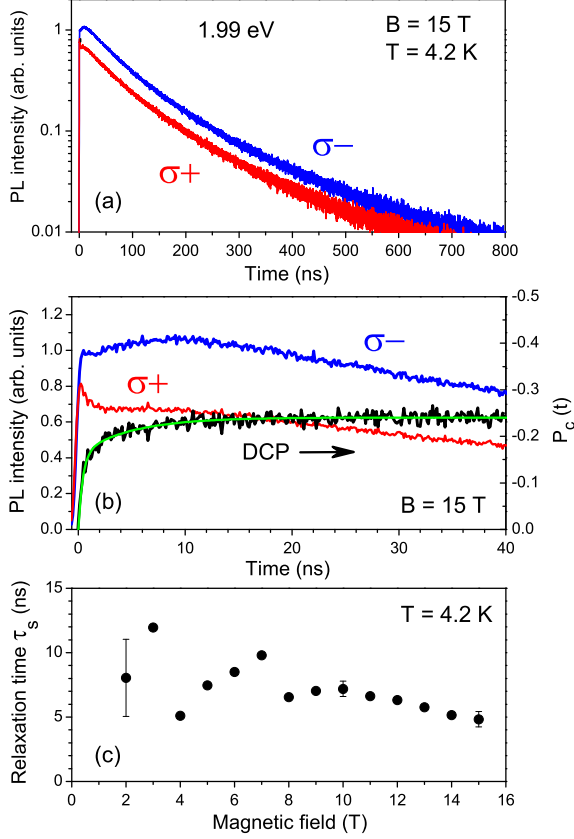


FIG. 3: Exciton spin dynamics of 3.4 nm CdTe NCs. The two upper panels give the recombination dynamics of the two circularly polarized components measured at the PL maximum for  $B = 15$  T, shown in (a) on a logarithmic scale for an extended time interval and in (b) on a linear scale for the initial time interval, along also with the DCP obtained from these data. (c) Magnetic field dependence of the exciton spin relaxation time evaluated from the DCP dynamics. The times for the slower component obtained from bi-exponential fits of the DCP dynamics are shown.

The experimental data for the exciton spin dynamics are collected in Fig. 3. There the recombination dynamics of the two circularly polarized components measured at the PL band maximum (1.99 eV) at  $B = 15$  T are shown in panel (a). One can see, that an intensity difference between the components is established shortly after the excitation pulse, after which the two signals decay roughly parallel to each other. The initial dynamics during 40 ns is shown in more detail in Fig. 3(b) together with the resulting DCP dynamics determined after Eq. (1). The small rise in PL intensity observed for the  $\sigma^-$  polarization during initial 10 ns is due to the energy transfer, see Ref. [32] for details. The DCP given by the

black line has a fast initial increase from zero up to about  $-0.15$  within times shorter than 1 ns, which is below the time resolution of the used experimental setup. It is followed by a slower increase reaching  $-0.25$  at 40 ns and  $-0.28$  up to one microsecond. From the bi-exponential fit shown by the green line in Fig. 3(b) we evaluate a slow spin relaxation time of 5 ns at  $B = 15$  T. The bi-exponential fit was done with the function

$$P_c(t) = P_c^{\text{eq}}(B) [1 - \exp(-t/\tau_s)] + A [\exp(-t/\tau_s) - \exp(-t/\tau_{\text{fast}})], \quad (4)$$

where the first term describes the emergence of DCP towards its equilibrium value  $P_c^{\text{eq}}$  and the second term describes its fast initial rise with a characteristic time  $\tau_{\text{fast}}$  for times shorter than  $\tau_A$ .

The magnetic field dependence of the slow spin relaxation time  $\tau_s$  is plotted in Fig. 3(c). It shows a steady decrease with increasing magnetic fields from about 10 ns down to 5 ns. Note that in weak magnetic fields the error bars for the data are larger, as the DCP values become smaller. The accuracy of the method improves at higher magnetic fields. The spectral dependence of the DCP rise time is rather weak, e.g., at  $B = 15$  T it varies from 4.5 ns at the high energy flank up to 5.5 ns at the low energy flank of the PL band.

The DCP dynamics consisting of the fast and slow components can be explained by the spin relaxation contributions of the bright and dark excitons. The fast component with the spin relaxation time shorter than 1 ns is provided by the bright exciton relaxation. This process is ultimately limited by the lifetime of the bright exciton, which can be as short as 2 ns. Therefore, the slow spin dynamics with flip times of 5-10 ns can be provided only by spin relaxation of the dark excitons. Note that this spin relaxation time is considerably shorter than the dark exciton lifetime of 150-260 ns. For this condition ( $\tau_s \ll \tau_F$ ) the experimentally measured DCP under CW excitation  $P_c(B)$  as used in Fig. 1(d) coincides with the equilibrium spin polarization  $P_c^{\text{eq}}(B)$ .

#### IV. MODELING AND DISCUSSION

Before we turn to the theoretical model, let us briefly summarize the experimental results. We have shown that in CdTe NCs the magnetic-field-induced circular polarization of PL reaches a saturation level of about  $-0.30$  at  $T = 4.2$  K. The spin relaxation time of the dark excitons is considerably shorter than its lifetime ( $\tau_s \ll \tau_F$ ), so that the polarization under CW excitation shown in Fig. 1(d) corresponds to the thermal equilibrium population of the exciton Zeeman levels. The strong dependence of the recombination dynamics on magnetic field evidences that most of the NCs have a quantization axis due to geometry deviation from the spherical shape.

One of the experimental results that we need to explain is the rather low saturation level of  $P_c = -0.30$  in the



limit of high magnetic fields. Depending on the NC spin structure that is determined, e.g., by the NC nonspherical shape, different levels of DCP saturation are expected:

(i) In prolate CdTe NCs, the exciton fine structure is similar to that of spherical or oblate hexagonal CdSe NCs. The lowest exciton state is the dark exciton with spin projections on the quantization axis  $\pm 2$ , while the states  $\pm 1^L$  (here the bright exciton due to the anisotropy induced admixture of the  $\pm 1^U$  state) and  $0^L$  are shifted to higher energies [13, 18, 24]. If the condition  $\tau_s \ll \tau_F$  is fulfilled, then the DCP of the dark exciton is determined only by its Zeeman splitting and the temperature. The DCP saturation level in high magnetic fields should be  $\pm 0.75$  and may become reduced to  $\pm 0.625$  in case of strong nonradiative recombination [14], here the sign of DCP depends on the exciton  $g$ -factor. In the other limiting case  $\tau_s \gg \tau_F$  or in the intermediate cases the value of time-integrated DCP will be reduced by the dynamical factor of the dark exciton  $d_F = \tau_F/(\tau_F + \tau_s)$ . However, the relaxation from bright to dark exciton might transfer the exciton polarization gained during the relaxation of the bright exciton to the polarization of the dark exciton and thus contribute to the observed DCP. This situation has not been considered theoretically up to now.

(ii) In oblate CdTe NCs the dark exciton ground state has spin  $0^L$  [13, 24] and, therefore, does not split in external magnetic field. As long as this state is the lowest one, i.e. it is not crossed by the next lying bright exciton state with  $\pm 1^L$  that becomes split with increasing magnetic field, the DCP value is zero.

In the following, we first revisit the case of prolate NCs and show that even when accounting for the four level system with a transfer of spin polarization from bright to dark excitons the saturation DCP level does not significantly reduce. Therefore, none of the considered scenarios can explain our experimental data. The small saturation level of  $P_c^{int}$  can, however, be explained by a model suggesting that the NC ensemble consists of a mixture of prolate and oblate NCs.

In nonspherical prolate CdTe NCs, the total angular momentum of the hole is aligned along the quantization axis originating from the shape anisotropy. Due to the exchange interaction between electron and hole, the electron spin becomes also pinned along this quantization axis. As a result the exciton  $g$ -factors for both dark and bright excitons are anisotropic and the exciton Zeeman splittings depend on the angle between the quantization axis and the magnetic field direction. Since the quantization axis is randomly oriented, the DCP of an ensemble of NCs has to be integrated over all angles. The recombination time of the dark exciton, being controlled by the dark-bright mixing of the exciton states, also depends on the magnetic field strength and on the NC orientation relative to the field direction. This may change the relative contribution of differently oriented NCs to the integral PL intensity and to the DCP signal in case of significant nonradiative recombination. The way to account for such contribution has been suggested in Ref. [14]. We extend

this approach for the case of a four level exciton structure with spin-dependent relaxation from bright to dark exciton.

Details of the four level model are given in the Appendix. The time-integrated DCP of an ensemble of randomly oriented, prolate CdTe NCs can be described by

$$P_c^{int}(B, T) = - \frac{\int_0^1 2x \rho^{int}(B, x, T) \eta_p(B, x) dx}{\int_0^1 (1 + x^2) \eta_p(B, x) dx}, \quad (5)$$

where

$$\rho^{int} = \rho_F(B, x, T) d_F + (1/2) \rho_A(B, x, T) d_A (1 - d_F). \quad (6)$$

Here  $d_A = \tau_A/(\tau_A + \tau_{sA})$  is the dynamical factor of the bright exciton,  $\eta_p = [1 + \tau_r/\tau_{nr}]^{-1}$  is the quantum efficiency of the prolate CdTe NCs [14], ( $\tau_r$  and  $\tau_{nr}$  are the radiative and nonradiative decay times of the dark exciton in prolate dots).  $x = \cos \Theta$ , where  $\Theta$  is the angle between the NC quantization axis and the magnetic field direction. We have introduced two equilibrium polarizations of bright and dark exciton populations  $\rho_{A(F)}(B, x, T) = \tanh(\Delta E_{A(F)}/2k_B T) = \tanh(g_{A(F)} \mu_B B x / 2k_B T)$ , controlled by the bright,  $g_A$ , and dark,  $g_F$ , exciton  $g$ -factors. Eq. (6) is derived for the case of equal initial population of bright and dark exciton states and the extreme case of spin dependent relaxation between bright and dark excitons (see Appendix).

The Eq. (6) has been obtained for the case  $k_B T \ll \Delta_{AF}$ , where  $\Delta_{AF}$  is the zero field splitting between the bright and dark excitons (a more general consideration will be presented elsewhere). Note, that if the bright and dark exciton  $g$ -factors have different signs the contributions from the bright and dark exciton polarizations may partly compensate each other. However, as we have already established the relatively fast spin relaxation for the dark exciton in experiment, its dynamical factor  $d_F \approx 1$  and, therefore, no contribution from the bright exciton to the DCP is expected.

Thus to explain the experimentally observed low saturation level of DCP at high magnetic fields we suggest that there is a subset of oblate NCs in the NC ensemble. It is important to note, that for such NCs the nonzero recombination rate of the dark  $0^L$  exciton state in zero magnetic field is due to the admixture of bright exciton states, either  $1^{L,U}$  or  $0^U$ . The rate can be accelerated by a magnetic field component perpendicular to the anisotropy axis due to the field-induced admixture of the  $1^L$  states [24]. (We assume that the Zeeman energy is much smaller than the energy separation to the upper bright exciton states.) Thus no strong difference between the magnetic field dependences of the recombination dynamics is expected for prolate and oblate NCs and the presence of both kinds of NCs leads to additional independent contributions to the multi-exponent emission decay only.

Since the exciton ground state of oblate CdTe NCs does not split in magnetic field, such NCs contribute only to the total PL intensity and give no DCP signal. Then,

the time-integrated DCP  $P_c^{\text{int}}(B)$  of an ensemble consisting of CdTe NCs with oblate and prolate shapes can be written as:

$$P_c^{\text{int}}(B, T) = - \frac{\int_0^1 2x\rho_F(B, x, T)\eta_p(B, x)dx}{\int_0^1 (1+x^2)[\eta_p(B, x) + q\eta_o(B, x)]dx}, \quad (7)$$

where  $q$  is the ratio of the number of oblate to prolate NCs, and  $\eta_o = [1 + \tau_r^o/\tau_{nr}^o]^{-1}$  is the quantum efficiency of oblate NCs ( $\tau_r^o$  and  $\tau_{nr}^o$  are the radiative and nonradiative decay times of the dark exciton in oblate NCs).

Next, we discuss two extreme cases and use them for fitting the experimental data in Fig. 1(d). First, in the limit of high quantum yield for both prolate and oblate NCs we put  $\eta_p = \eta_o \approx 1$ . Then, Eq. (7) reduces to

$$P_c^{\text{int}}(B, T) = - \frac{\int_0^1 2x\rho_F(B, x, T)dx}{(1+q)\int_0^1 (1+x^2)dx}. \quad (8)$$

The time-integrated DCP measured at the three explored temperatures can be fitted well using Eq. (8) (see red lines in Fig. 1(d)) with two fitting parameters:  $q = 1.5$  and  $g_F = 2.4$ . It is worth to note that not only the absolute value but also the sign of the exciton  $g$ -factor can be obtained from our experiment, as it is closely connected to the DCP sign.

Second, in the limit of low quantum yield ( $\tau, \tau^o \gg \tau_{nr}$ ) at zero magnetic field, one can assume the quantum efficiency of prolate (oblate) dots gained in magnetic field to be  $\eta_{p(o)}(1-x^2)B^2$  [14]. Then, Eq. (7) reduces to

$$P_c^{\text{int}}(B, T) = - \frac{\int_0^1 2x\rho_F(B, x, T)(1-x^2)dx}{(1+q\eta_o/\eta_p)\int_0^1 (1+x^2)(1-x^2)dx}. \quad (9)$$

Fitting the experimental data in Fig. 1(d) with Eq. (9) gives  $g_F = 2.9$ , which is close to the first limiting case of 2.4 and  $q\eta_o/\eta_p = 1$ .

By comparing these two extreme cases, we conclude that the dark exciton  $g$ -factor in 3.4 nm-diameter CdTe NCs is in the range from 2.4 to 2.9. Its positive sign corresponds to the observed negative circular polarization induced by the magnetic field. The obtained value is in good agreement with theoretical estimations of the dark exciton  $g$ -factor of 3.7 according to  $g_F = g_e - 3g_h$  [13, 24], where  $g_e$  and  $g_h$  are the electron and hole  $g$ -factors. In bulk CdTe  $g_e = -1.6$ , however, due to the strong quantum confinement in 3.4 nm NCs it becomes positive and we estimate its value using the theory developed in Ref. [33] to be  $g_e = 0.7$ . The hole  $g$ -factor is

estimated using the expression developed for a potential of spherical symmetry (see Refs. [13, 24, 34]) as  $g_h = -1$ . All material parameters used for the calculations were taken from Ref. [35]. The fact that we obtain from our fitting a value of the exciton  $g$ -factor, that is expected for the dark exciton, approves our assignment of the slow component in the DCP dynamics to the dark exciton.

The measured values of the spin relaxation times of 5-10 ns for the dark excitons in CdTe NCs are longer than the spin relaxation times reported earlier for CdSe/ZnS NCs [14, 15], where times shorter than one ns were found at  $B = 12$  T and for CdSe/CdS NCs with CdS shells thinner than 4 nm [16]. Note, that in CdSe/CdS NCs with shells thicker than 5 nm the emission is dominated by negatively charged excitons (trions) having rather long spin relaxation times up to 60 ns, measured at  $B = 1$  T and  $T = 4.2$  K [16].

In small neutral colloidal NCs, the exciton spin relaxation between the  $\pm 1^L$  states is mainly driven by the long-range electron-hole exchange interaction and by the exciton-phonon interaction [36–38]. For the dark exciton the relaxation between the  $\pm 2$  sublevels may be caused by the same mechanisms considering the admixture of the  $\pm 1^L$  states. This explains the longer spin relaxation within the dark exciton doublet compared to the bright excitons and its acceleration in magnetic field.

To summarize, the exciton recombination and spin relaxation dynamics have been studied experimentally for colloidal CdTe NCs at cryogenic temperatures and in high magnetic fields. The strong modification of the recombination dynamics in magnetic field evidences that the studied NCs have a structural quantization axis being either prolate or oblate in shape. This conclusion is confirmed by the low saturation level of the magnetic-field-induced circular polarization of the exciton emission. The spin dynamics of the dark excitons happen in the range of 5-10 ns with a considerable shortening with increasing magnetic field. The exciton  $g$ -factor of 2.4-2.9 evaluated from fitting the experimental data in the frame of the suggested approach is in good agreement with the value expected for the dark excitons in CdTe NCs.

**Acknowledgment.** The authors are thankful to Al. L. Efros and L. Biadala for stimulating discussions. This work was supported by the EU Seventh Framework Programme (Grant No. 237252, Spin-Optronics), the Deutsche Forschungsgemeinschaft, the MERCUR and by the Research Grant Council of Hong Kong S.A.R. (project No.[T23-713/11]). A.V.R. acknowledges support from the Russian Foundation for Basic Research (Grant No. 13-02-00888-a).

- 
- [1] Z. Tang, N. A. Kotov and M. Giersig, *Science* **297**, 237 (2002).  
 [2] N. Gaponik, D. V. Talapin, A. L. Rogach, K. Hoppe, E. V. Shevchenko, A. Kornowski, A. Eychmuller, and H. Weller, *J. Phys. Chem. B* **106**, 7177 (2002).

- [3] J. Byrne, Y. Williams, A. Davies, S. A. Corr, A. Rakovich, Y. K. Gun'ko, Y. P. Rakovich, J. F. Donegan and Y. Volkov, *Small*, **3**, 1152 (2007).  
 [4] A.L. Rogach, T. Franzl, T.A. Klar, J. Feldmann, N. Gaponik, V. Lesnyak, A. Shavel, A. Eychmuller, Y.P.

- Rakovich, and J.F. Donegan, J. Phys. Chem. C **111**, 14628 (2007).
- [5] A. L. Rogach, Nano Today **6**, 355 (2011).
- [6] Y. Zhang, L. Mi, J.-Y. Chen, and P.-N. Wang, Biomed. Mater. **4**, 012001 (2009).
- [7] J. Lovric, S. J. Cho, F. M. Winnik, and D. Maysinger, Chemistry & Biology **12**, 1227 (2005).
- [8] G. Han, T. Mokari, C. Ajo-Franklin, and B. E. Cohen, J. Am. Chem. Soc. **130**, 15811 (2008).
- [9] A. L. Rogach, M. Ogris, Current Opinion Mol. Therap. (12), 331 (2010).
- [10] *Spin Physics in Semiconductors*, edited by M. I. Dyakonov (Springer-Verlag, Berlin, 2008).
- [11] D.P. Di Vincenzo, D. Bacon, J. Kempe, G. Burkard, K.B. Whaley, Nature **408**, 339 (2000).
- [12] A. Glozman, E. Lifshitz, K. Hoppe, A.L. Rogach, H. Weller, A. Eychmuller, Israel J. Chem. **41**, 39 (2001).
- [13] Al. L. Efros, M. Rosen, M. Kuno, M. Nirmal, D. J. Norris, and M. Bawendi, Phys. Rev. B **54**, 4843 (1996).
- [14] E. Johnston-Halperin, D. D. Awschalom, S. A. Crooker, Al. L. Efros, M. Rosen, X. Peng, and A. P. Alivisatos, Phys. Rev. B **63**, 205309 (2001).
- [15] M. Furis, J. A. Hollingsworth, V. I. Klimov, and S. A. Crooker, J. Phys. Chem. B **109**, 15332 (2005).
- [16] F. Liu, L. Biadala, A.V. Rodina, D.R. Yakovlev, D. Dunker, C. Javaux, J.-P. Hermier, Al.L. Efros, B. Dubertret, and M. Bayer, Phys. Rev. B **88**, 035302 (2013).
- [17] R. D. Schaller, S. A. Crooker, D. A. Bussian, J. M. Pietryga, J. Joo, and V. I. Klimov, Phys. Rev. Lett. **105**, 067403 (2010).
- [18] J.H. Blokland, V.I. Claessen, F.J.P. Wijnen, E. Groeneweld, C. de Mello Donegá, D. Vanmaekelbergh, A. Meijerink, J.C. Maan, and P.C.M. Christianen, Phys. Rev. B **83**, 035304 (2011).
- [19] F. J. P. Wijnen, J. H. Blokland, P. T. K. Chin, P. C. M. Christianen, and J. C. Maan, Phys. Rev. B **78**, 235318 (2008).
- [20] D. E. Blumling, T. Tokumoto, S. McGill, and K. L. Knappenberger, J. Phys. Chem. C **115**, 14517 (2011).
- [21] J. A. Gupta, D. D. Awschalom, Al. L. Efros, and A. V. Rodina, Phys. Rev. B **66**, 125307 (2002).
- [22] D. Dunker, T. S. Shamirzaev, J. Debus, D. R. Yakovlev, K. S. Zhuravlev, and M. Bayer, Appl. Phys. Lett. **101**, 142108 (2012).
- [23] Note that in Refs. 14, 15, 20 different definition of  $P_c$  has been used, namely  $P_c = (I^- - I^+) / (I^- + I^+)$ , which gives inverted sign for DCP compared to the definition used here.
- [24] Al. L. Efros, Fine Structure and Polarization Properties of Band-Edge Excitons in Semiconductor Nanocrystals; Chapter 3; pp. 103-141 in *Semiconductor and Metal Nanocrystals: Synthesis and Electronic and Optical Properties*; editors V. I. Klimov and M. Dekker (New York, 2003).
- [25] S. Shanbhag, and N. A. Kotov, J. Phys. Chem. B **110**, 12211 (2006).
- [26] Z. Tang, Z. Zhang, Y. Wang, S.C. Glotzer, and N. A. Kotov, Science **314**, 274 (2006).
- [27] *Optical Orientation*, edited by F. Meier and B. P. Zakharchenya (North-Holland, Amsterdam, 1984).
- [28] A. L. Rogach, T. A. Klar, J. M. Lupton, A. Meijerink, J. Feldmann, J. Mater. Chem. **19**, 1208 (2009).
- [29] S.F. Wuister, R. Koole, C.D. Donega, and A. Meijerink, J. Phys. Chem. B **109**, 5504 (2005).
- [30] M. Lunz, A.L. Bradley, W.-Y. Chen, V.A. Gerard, S.J. Byrne, Y.K. Gunko, V. Lesnyak, and N. Gaponik, Phys. Rev. B **81**, 205316 (2010).
- [31] D.E. Blumling, T. Tokumoto, S. McGill, and K.L. Knappenberger, Phys. Chem. Chem. Phys. **14**, 11053 (2012).
- [32] F. Liu, A.V. Rodina, D.R. Yakovlev, A. Greulich, E. D. Vakhtin, A. Susha, A. L. Rogach, Y. G. Kusraev, and M. Bayer, to be published.
- [33] A.V. Rodina, Al.L. Efros, and A.Y. Alekseev, Phys. Rev. B **67**, 155312 (2003).
- [34] B.L. Gelmont, and M.I. Dyakonov, Sov. Phys. Semicond. **7**, 1345 (1973).
- [35] G.N. Aliev, O.S. Koshchug, A.I. Nesvizhskii, R.P. Seisyan, and T.V. Yazeva, Phys. Solid State **35**, 764 (1993).
- [36] G.D. Scholes, J. Kim, and C.Y. Wong, Physical Review B **73**, 195325 (2006).
- [37] T. Takagahara, Phys. Rev. B **62**, 16840 (2000).
- [38] H. Ma, Z. Jin, Z.B. Zhang, G.F. Li, and G.H. Ma, J. Phys. Chem. A **116**, 2018 (2012).
- [39] V.I. Klimov, J. Phys. Chem. B **104**, 6112 (2000).

## Appendix

Here we consider a four-level system for the exciton in magnetic field with populations  $N_A^\pm(t)$  (bright exciton Zeeman states) and  $N_F^\pm(t)$  (dark exciton Zeeman states). The rate equations for  $N_A^\pm(t)$  and  $N_F^\pm(t)$  are

$$\begin{aligned} \frac{dN_A^+}{dt} = & -N_A^+(\Gamma_A + \gamma_A^+ + \gamma_0 + \gamma_{th}^+) + N_A^- \gamma_A^- + N_F^+ \gamma_{th}^+ \\ & + G(t), \end{aligned} \quad (10)$$

$$\begin{aligned} \frac{dN_A^-}{dt} = & -N_A^-(\Gamma_A + \gamma_A^- + \gamma_0 + \gamma_{th}^-) + N_A^+ \gamma_A^+ + N_F^- \gamma_{th}^- \\ & + G(t), \end{aligned} \quad (11)$$

and

$$\begin{aligned} \frac{dN_F^+}{dt} = & -N_F^+(\Gamma_F + \gamma_F^+ + \gamma_{th}^+) + N_F^- \gamma_F^- + N_A^+(\gamma_0 + \gamma_{th}^+) \\ & + G(t), \end{aligned} \quad (12)$$

$$\begin{aligned} \frac{dN_F^-}{dt} = & -N_F^-(\Gamma_F + \gamma_F^- + \gamma_{th}^-) + N_F^+ \gamma_F^+ + N_A^-(\gamma_0 + \gamma_{th}^-) \\ & + G(t). \end{aligned} \quad (13)$$

Here  $\Gamma_{A(F)}$  are the bright and dark exciton recombination rates (comprising radiative,  $\Gamma_{A(F)}^r$ , and nonradiative,  $\Gamma_{A(F)}^{nr}$ , recombination),  $\gamma_0$  is the relaxation rate from bright exciton to dark exciton at zero temperature, and  $\gamma_{th}^\pm$  takes into account thermally-induced mixing of bright and dark states. These rates are related to the exciton lifetimes by  $1/\tau_F = \Gamma_F$  and  $1/\tau_A = \Gamma_A + \gamma_0$ . We consider only the extreme cases of spin dependent relaxation in which only the process between the  $N_A^+$  and  $N_F^+$  states (or the  $N_A^-$  and  $N_F^-$  states) are possible, both at zero temperature and thermally induced at elevated temperature. For these processes only the flip of the electron spin is required, which can be provided via interaction with

acoustic phonons (in one-phonon processes) or via interaction with surface localized spins. The cross-relaxation processes between the  $N_A^+$  and  $N_F^-$  states (or the  $N_A^-$  and  $N_F^+$  states) require the flip of the heavy-hole spin 3/2 and, therefore, are considerably slower [16]. The spin relaxation times for the bright and dark excitons are

$$\frac{1}{\tau_{sA}} = \gamma_A^+ + \gamma_A^-, \quad \frac{1}{\tau_s} = \gamma_F^+ + \gamma_F^-. \quad (14)$$

Here we will consider only the case of low temperatures  $k_B T \ll \Delta_{AF} \pm 1/2(g_A - g_F)\mu_B B$ , where  $\Delta_{AF}$  is the zero field splitting between bright and dark excitons, and assume that  $1/2|(g_A - g_F)\mu_B B| < \Delta_{AF}$ . This allows us to neglect the thermally-induced mixing between bright and dark exciton states and put  $\gamma_{th}^\pm = 0$ , while thermalization between the Zeeman levels of the bright (dark) excitons is taken into account. A more general consideration will be published elsewhere.

The excitation term  $G(t)$  describes the unpolarized equal intensity pumping of bright and dark exciton states. Such pumping corresponds to our experimental conditions: nonresonant excitation well above the exciton energy and fast relaxation of hot excitons to the ground state, assisted by optical phonons and interaction with the surface [39]. For short pulse excitation one may assume  $G(t) = 0$  and complete the model by assuming the initial conditions  $N_A^+(0) = N_A^-(0) = N_F^+(0) = N_F^-(0) = N_0/4$ , where  $N_0$  is the total number of nanocrystals with exciton energy such that it can be excited by the laser pulse. For CW excitation  $G(t) = G$ . We have determined the solutions below for the case of CW excitation.

To obtain these steady state solutions we take  $dN_F^+/dt = dN_F^-/dt = dN_A^+/dt = dN_A^-/dt = 0$  and solve the system of four linear equations for  $N_A = N_A^+ + N_A^-$ ,  $N_F = N_F^+ + N_F^-$ ,  $\Delta N_A = N_A^+ - N_A^-$  and  $\Delta N_F = N_F^+ - N_F^-$ :

$$\frac{N_A}{N} = \frac{\Gamma_F}{2\gamma_0 + \Gamma_A + \Gamma_F}, \quad (15)$$

$$\frac{N_F}{N} = \frac{\Gamma_A + 2\gamma_0}{2\gamma_0 + \Gamma_A + \Gamma_F}, \quad (16)$$

$$\frac{\Delta N_A}{N} \approx \frac{\Gamma_F}{2\gamma_0} \rho_A d_A, \quad (17)$$

$$\frac{\Delta N_F}{N} \approx \left( \rho_F d_F + \frac{1 - d_A}{2} \rho_A \right), \quad (18)$$

where  $N = N_A + N_F = G\tau_F(2 - \tau_A\Gamma_A) + G\tau_A$  and we used the relations  $\gamma_0 \gg \Gamma_A \gg \Gamma_F$  to approximate the solutions. One can see, that under these conditions and for  $k_B T \ll \Delta_{AF}$  the population of the bright exciton state is much smaller than for the dark exciton state:  $N_A \ll N_F$  and  $\Delta N_A \ll \Delta N_F$ .

Following the theory of Refs. [14, 24] we assume that the polarization properties of the  $\pm 2$  dark exciton recombination are determined solely by coupling with the  $\pm 1$  bright excitons. We obtain for the intensities of the  $\sigma^+$  and  $\sigma^-$  polarized PL:

$$I^+ + I^- = 2(1 + x^2)(\eta_A N_A + \eta_F N_F), \quad (19)$$

$$I^+ - I^- = 4x(\eta_A \Delta N_A + \eta_F \Delta N_F), \quad (20)$$

where  $x = \cos \Theta$  and  $\eta_{A(F)} = [1 + \Gamma_{A(F)}^{nr}/\Gamma_{A(F)}^r]^{-1}$  are the quantum efficiencies of the bright and dark excitons. One can see, that if  $\eta_A \approx \eta_F$ , the contribution from  $N_A$  and  $\Delta N_A$  to the DCP can be neglected. We arrive at an expression for the DCP under CW excitation (which is equivalent to the time-integrated DCP) given by Eqs. (5) and (6), where the quantum efficiency of the prolate NCs  $\eta_p$  corresponds to  $\eta_F$ .